AGU PUBLICATIONS

JGR

Journal of Geophysical Research: Planets

RESEARCH ARTICLE
10.1002/2017JE005304

Key Points:
- A seasonal MIV-generated CaO exosphere with maximum density above the dawnside-nightside hemisphere of Mercury is expected
- An exospheric energetic Ca component, derived from the dissociative ionization and neutralization of CaO, is expected above the same region
- Simulated Ca distribution in good agreement with the MESSENGER observations; the derived emission rate is up to 1/10 of the observed one

Correspondence to:
C. Plainaki,
christina.plainaki@asi.it

Citation:
Plainaki, C., A. Mura, A. Milillo, S. Orsini, S. Livi, V. Mangano, S. Massetti, R. Rispoli, and E. De Angelis (2017), Investigation of the possible effects of comet Encke's meteoroid stream on the Ca exosphere of Mercury, *J. Geophys. Res. Planets*, *122*, 1217–1226, doi:10.1002/2017JE005304.

Received 10 MAR 2017
Accepted 11 MAY 2017
Accepted article online 15 MAY 2017
Published online 3 JUN 2017

Investigation of the possible effects of comet Encke's meteoroid stream on the Ca exosphere of Mercury

Christina Plainaki[1], Alessandro Mura[2], Anna Milillo[2], Stefano Orsini[2], Stefano Livi[3], Valeria Mangano[2], Stefano Massetti[2], Rosanna Rispoli[2], and Elisabetta De Angelis[2]

[1]Agenzia Spaziale Italiana, Rome, Italy, [2]IAPS, INAF, Rome, Italy, [3]Southwest Research Institute, San Antonio, Texas, USA

Abstract The MErcury Surface, Space ENvironment, GEochemistry, and Ranging (MESSENGER) observations of the seasonal variability of Mercury's Ca exosphere are consistent with the general idea that the Ca atoms originate from the bombardment of the surface by particles from comet 2P/Encke. The generating mechanism is believed to be a combination of different processes including the release of atomic and molecular surface particles and the photodissociation of exospheric molecules. Considering different generation and loss mechanisms, we perform simulations with a 3-D Monte Carlo model based on the exosphere generation model by Mura et al. (2009). We present for the first time the 3-D spatial distribution of the CaO and Ca exospheres generated through the process of micrometeoroid impact vaporization, and we show that the morphology of the latter is consistent with the available MESSENGER/Mercury Atmospheric and Surface Composition Spectrometer observations. The results presented in this paper can be useful in the exosphere observations planning for BepiColombo, the upcoming European Space Agency-Japanese Aerospace Exploration Agency mission to Mercury.

1. Introduction and Motivation for the Current Work

Mercury's calcium exosphere was discovered through ground-based telescope measurements [*Bida et al.*, 2000] and further detected by the Ultraviolet and Visible Spectrometer (UVVS), one component of the Mercury Atmospheric and Surface Composition Spectrometer (MASCS) instrument [*McClintock and Lankton*, 2007] onboard MErcury Surface, Space ENvironment, GEochemistry, and Ranging (MESSENGER) spacecraft [*Solomon et al.*, 2007]. *Burger et al.* [2014] analyzed the Ca measurements obtained over eight Mercury years with MASCS/UVVS during MESSENGER's primary and first extended missions (March 2011 to March 2013) and simulated exospheric processes that could be responsible for the Ca distribution and seasonal variability. They showed that there is a persistent source of energetic calcium located in the dawn equatorial region and a seasonal dependence in the calcium source rate, peaking at ~20° True Anomaly Angle (TAA). No obvious year-to-year variations in the near-surface dayside calcium exosphere were found. These recent MESSENGER data revealed also that exospheric Ca is (a) extremely hot, (b) seen almost exclusively on the dawnside of the planet, and (c) its content varies seasonally, not sporadically [*Killen*, 2016].

Although *Burger et al.* [2014] did not determine the mechanism responsible for ejecting calcium from Mercury's surface to the exosphere they argued that among all candidate processes, the molecular dissociation of Ca-bearing molecules produced in micrometeoroid impact vaporization (MIV) of surface material appears to be the most consistent one with their analysis with respect to both the energy spectrum and spatial distribution. In this context, *Killen and Hahn* [2015] suggested that the observed seasonal variations in Mercury's calcium exosphere may be attributed to the release of Ca-bearing molecules following the bombardment of Mercury's surface by the variable influx of interplanetary dust. In particular, the persistent enhancement found in the MASCS data at TAA ~20° was attributed by *Killen and Hahn* [2015] to the vaporization of surface material induced by the impact of a meteor stream, possibly resulting from Comet Encke. *Christou et al.* [2015] tested this hypothesis through simulations of the dynamical evolution of Encke particles under planetary perturbations and Poynting-Robertson drag. They found that millimeter-sized grains forming the stream of meteoroids ejected $1–2 \cdot 10^4$ years ago from comet Encke impact the surface at Mercury when the planet is near TAA ~25°. The observed excess emission was consistent with a major dust release episode 10 kyr ago, possibly due to Encke progenitor breakup.

The physical state of the MIV ejecta has not yet been determined through in situ measurements at Mercury, since, up to now, there has not been any possibility of such molecular in situ detection. Currently, only

assumptions have been used for the composition of the released gas upon meteoroid impact on Mercury's surface. Ca-bearing molecules in impact vapor plumes are more likely to be produced than Ca atoms [*Berezhnoy and Klumov*, 2008]. These molecules get dissociated quickly [*Berezhnoy and Klumov*, 2008; *Berezhnoy*, 2013] releasing energetic Ca atoms [*Burger et al.*, 2014; *Christou et al.*, 2015; *Killen*, 2016; *Killen et al.*, 2005]. Such a scenario would be consistent with recent observations and models of micrometeoroids at Earth showing that there is a strong dawn enhancement in the impactor flux [*Janches et al.*, 2006; *Pifko et al.*, 2013]. However, *Burger et al.* [2014] noted that it is not yet clear whether molecular dissociation produces atomic Ca with an effective temperature >50,000 K or not. Recently, *Killen* [2016] used estimations by *Berezhnoy and Klumov* [2008] to study the equilibrium between the various calcium-bearing ejecta as a result of impact of a CI meteorite onto Mercury. For the Mercurian regolith an elemental composition of ~90% plagioclase and 10% pyroxene by volume was assumed. Since, at temperatures above 3750 K, CaO dominates over both atomic Ca and $Ca(OH)_2$, *Killen* [2016] considered that the predominant form of the initial Calcium ejecta is CaO and examined different mechanisms that could lead to the production of an energetic Ca cloud from the MIV-generated vapor. They showed that a mean velocity induced from impact shocks of about 15 km/s would be consistent with a temperature for the exospheric species of 54,000 K which is within the uncertainties of the value of ~70,000 K, estimated by *Burger et al.* [2014], on the basis of MASCS/UVVS data. It is emphasized that MIV, as well as other surface release processes (e.g., photon-stimulated desorption, electron-stimulated desorption, and sputtering), produces in general cooler ejecta [*Killen and Ip*, 1999; *Killen et al.*, 2007; *Killen*, 2016]. To solve the problem of Ca energization, *Killen* [2016] proposed a two-step process in which the initial process (i.e., MIV) ejects calcium-bearing molecules and a second almost instant process (i.e., dissociative ionization and neutralization) produces highly energetic atomic Ca. Assuming even a conservative impact velocity distribution of about 40 km/s [*Cintala*, 1992], the generated Ca atoms could have velocities peaking near 20 km/s resulting in equivalent temperatures of ~64,000 K.

In view of the recent MESSENGER findings and the subsequent analyses, the aim of the present work is to provide a detailed Ca-source extraction model simulating the expected 3-D Ca density distribution in Mercury's exosphere due to the MIV mechanism. Using as an input the information on the arrival geometry of the Mercury-intercepting particles of comet Encke's meteoroid stream as estimated by *Christou et al.* [2015], we modify the exosphere generation model by *Mura et al.* [2009] in order to refine the implemented MIV process. In our model, described in section 2, we include the dissociation of Ca-bearing neutral molecules into fragments and we investigate the excess energies. In section 3, we provide for the first time the expected 3-D spatial distribution of Mercury's Ca exosphere generated after the surface's bombardment by meteoroids from the stream of comet Encke. In section 4, we examine its consistency with the available recent MESSENGER/MASCS observations discussed in *Killen and Hahn* [2015] and discuss the effect of different assumptions. Through our estimations, we aim to better constrain the size and variability of the source region providing information that may be of help during the planning of the observations by instruments onboard Bepi Colombo (e.g., Search for Exospheric Refilling and Emitted Natural Abundances/Start from a Rotating FIeld mass spectrOmeter (SERENA/STROFIO)). The summary and the conclusions of the current work are given in section 5.

2. Model Description and Assumptions

In the current study, we simulate the bombardment of Mercury's surface by particles of diameter equal to ~958 μm, ejected from comet Encke ~10 kyr ago, and hitting the surface at TAA ranging between 10° and 60° (population 1 in Figure 2, panel 1:1, in *Christou et al.* [2015]). We assume an initial fireball temperature equal to ~4000 K and a total stream mass influx, F, equal to 10.5 g s^{-1} [*Killen and Hahn*, 2015]. The numerical Ca abundance [Ca] for both the Encke meteoroids and Mercury surface is considered to be equal to 0.035 [*Killen*, 2016]. We note, however, that *Weider et al.* [2015] showed that the MESSENGER/X-Ray Spectrometer (XRS)-derived maps evidence surface regions (between 0° and 60° in latitude and 230° and 320° in longitude) which are by a factor of ~2 denser in Ca. Therefore, the results of the current simulations are a lower limit estimation: in the case that the meteoroid stream occurs in the high Ca-concentration region the expected release would double the exosphere generation rate.

The generation rate of the impact-vaporized mass is given as a function of the target (regolith) and projectile (meteoroid) properties [*Cintala*, 1992; *Mangano et al.*, 2007]:

$$\frac{dm_t}{dt} = \frac{\rho_t}{\rho_p}\frac{dm_p}{dt}\left(c + dv + ev^2\right) \quad (1)$$

where ρ_t and ρ_p are the densities of the target and projectile, respectively; $\frac{dm_p}{dt}$ is the stream mass influx on Mercury's surface; v is the approximate impact velocity; c, d, and e are parameters depending on the temperature of the soil and the composition of the projectile, here considered as in *Mangano et al.* [2007]: $c = -0.848$, $d = -0.0889$ km^{-1} s, and $e = 0.0217$ km^{-2} s^2.

In the current model the assumed exospheric population, released from the surface upon meteorite impact, includes mainly thermal CaO molecules, and to a much lesser extent (energetic) Ca and O components, generated through dissociative ionization [*Sidis*, 1989]. The shock-induced dissociative ionization followed by the fragment neutralization is a possible pathway explaining the production of at least a part of the observed hot exospheric Ca [*Killen*, 2016]. Since the neutralization should occur within nanoseconds after the initial impact, in our simulations we assume that energetic neutral Ca fragments are directly released upon the meteoroids' surface bombardment. The plasma expansion for impacts on uncharged tungsten has a distribution ranging between ~10 and 30 km/s, with a peak velocity of ~20 km/s [*Lee et al.*, 2012; *Starks et al.*, 2006]. Based on this information, here we assume that the energetic Ca velocity is equal to 20 km/s ($T \sim 70{,}000$ K). We note, however, that the energetic Ca source may not be thermal. Indeed, *Burger et al.* [2014] tested whether the UVVS data were consistent with an initial Gaussian speed distribution instead of a Maxwellian flux distribution. Unfortunately, these authors concluded that it was possible to constrain the source speed only for the dayside limb scan data, which were indeed consistent with a Gaussian speed distribution. Given this uncertainty, in the current study we choose to use a Maxwellian flux distribution for the energetic Ca component at $T \sim 70{,}000$ K.

Considering an impact velocity equal to 35 km/s and the impact directions estimated by *Christou et al.* [2015], the release rate for Ca (in Ca-bearing molecules), $F = \frac{dm_t}{dt}[\mathrm{Ca}]/m_{\mathrm{Ca}}$, is equal to $2.1 \cdot 10^{23}$ s^{-1}. This rate is slightly higher than the value estimated by *Christou et al.* [2015], equal to $0.69 \cdot 10^{23}$ s^{-1}, due to the different empirical models considered in each case (see equation (1)). If we assume that 0.85% of this vapor is ionized and dissociates [*Killen*, 2016] releasing Ca at high velocities, then the energetic Ca release rate upon impact becomes $1.8 \cdot 10^{21}$ s^{-1}.

In the current study, a meteoroid impact velocity equal to 35 km/s was considered. This value is within the range determined by the simulations of the dynamical evolution of Encke particles under planetary perturbations and Poynting-Robertson drag [*Christou et al.*, 2015]. In contrast to the so-called sporadic background where there is a distribution of impact velocities [see *Marchi et al.*, 2005], the impact velocity for cometary streams is virtually the same for all meteoroids within the same stream impacting a planet and are fairly well constrained from the simulations of *Christou et al.* [2015].

Note that a vaporized component due to MIV induced by meteoroids from the Dust Disk is also expected. The estimated released flux due to this population (this is the fraction of the impact vaporization flux of Ca-bearing minerals in all forms) at $0° < \mathrm{TAA} < 90°$ ranges between 0.6 and $0.75 \cdot 10^6$ cm^{-2} s^{-1} [*Killen and Hahn*, 2015]. This is translated (in units of release rate if multiplied with πR^2) to $1.1 \cdot 10^{19}$ s^{-1}. Therefore, it can be considered negligible with respect to the release caused by the impacts of comet Encke stream.

In summary, in the current model we assume an initial release rate for energetic (~20 km/s) Ca equal to ~$1.8 \cdot 10^{21}$ s^{-1} and an initial rate for thermal CaO (~4000 K) equal to $2.1 \cdot 10^{23}$ s^{-1}. We underline that these particles are assumed to be emitted from a specific area upon the surface extending from 5° to 23° in subradiant latitude (here defined as the latitude of the subradiant point on Mercury's surface) and from 145° to 175° in solar elongation (note that elong = 0° corresponds to the planet-Sun direction).

In our simulations, we take into account also the photodissociation of the initially released CaO molecules. This process populates the exosphere with thermal Ca and O atoms. The rate of CaO photodissociation has not yet been measured. The most optimistic production rate for Ca is consistent with the assumption of a photodissociation rate equal to the inverse of the photoionization lifetime. This results in a photodissociation rate equal to 7.4×10^{-4} s^{-1}. Nevertheless, for the measured Ca column density of $1.5 \cdot 10^8$ cm^{-2} [*Killen et al.*, 2005], the derived photodissociation rate is $7.5 \cdot 10^{-5}$ s^{-1} at perihelion and $6 \cdot 10^{-5}$ s^{-1} at aphelion. Given the configurations under study, which refer to orbital phases near the perihelion, we consider a

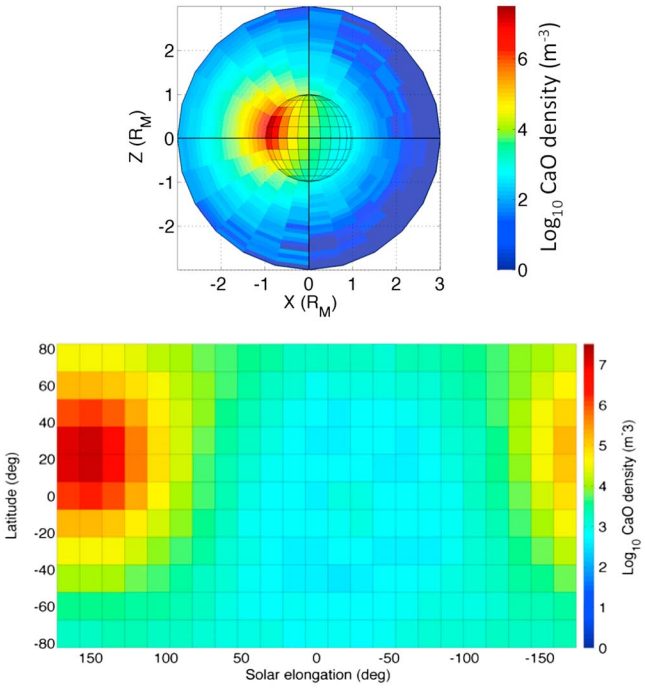

Figure 1. (top) Spatial distribution of the MIV-generated CaO density in the *x-z* plane, as seen from above the hemisphere centered at the dawn terminator. Positive *x* axis points to the Sun, whereas the *z* axis is the planet's spin axis.(bottom) Distribution of the MIV-generated CaO density near the surface. The subradiant solar elongation is 0° at the Sun-planet direction and dawn is at 90°.

photodissociation rate equal to $7.5 \cdot 10^{-5}$ s^{-1}. Photodissociation of CaO would result in an energy gain of about 0.8 eV for Ca, which would be consistent with a total velocity for Ca of ~2 km/s.

Finally, photoionization of all the exospheric species considered to be involved in this process (CaO, Ca, and O) is assumed. Below we focus in the Ca and Ca-bearing molecules. The Ca photoionization lifetime is $1.4 \cdot 10^4$ s at Earth [from *Huebner and Mukherjee*, 2011; *Killen and Hahn*, 2015]. At Mercury, the Ca photoionization lifetime varies from 23 min at perihelion to 52 min at aphelion [*Burger et al.*, 2014]. In the current simulations we have assumed a value of ~1740 s for the orbital phase where $0° < TAA < 90°$.

To simulate the Ca density in the exosphere of Mercury, we used a Monte Carlo model as in *Mura et al.* [2009]. The energy distribution of the emitted CaO and Ca particles was implemented with a Von Neumann algorithm. A large number ($>10^6$) of test particle trajectories were simulated; a weight factor *w* was associated to each test particle to reproduce the flux *F*. The trajectories were calculated using the classical equations of motion. The acceleration due to radiation pressure, unlike the case for sodium, can be neglected. The weight factor assigned to the Monte Carlo test particle is then adjusted to take into account photodissociation and photoionization: at each step, the probability for the Ca-bearing molecule to dissociate is calculated according to the position of the test particle (in daylight or in eclipse); with that same probability, the test particle may be turned into a Ca test particle.

We defined a 3-D spherical accumulation grid extending between 1 R_M and 3 R_M (100 radial steps, 12 latitudinal steps, and 24 longitudinal steps) and with R_M = 2439 km being the radius of Mercury. The Ca density inside one grid cell was calculated taking into account the number of test particles, the weight factor, and the lifetime inside the cell that each test particle actually experiences.

3. Results

In Figure 1 (top), the spatial distribution of the MIV-generated CaO exosphere is presented. Note that Figure 1 (top) refers to the Mercury solar orbital (MSO) coordinate system that is the Mercury equivalent of the geocentric-solar-ecliptic solar used at Earth. So in the MSO system, *x* is directed from the planet's center to the Sun, *y* is in the plane of Mercury's orbit and positive opposite to the planetary velocity vector, and *z* completes the right-handed system. Our results show that the region of the maximum flux of micrometeoroid impacts determines the actual shape of the neutral environment. Indeed, the CaO exosphere is denser above the midnight-to-dawn quadrant (subradiant solar elongation ranging from 90° to 180° in Figure 1, bottom) where the molecules are preferentially ejected into the exosphere by impact vaporization. According to the simulations, CaO densities up to $2 \cdot 10^7$ m^{-3} (see Figure 1, top) are expected near the surface, at the near-equatorial latitudes in the antisolar direction. The respective column density of the CaO component is up to $4 \cdot 10^8$ cm^{-2}.

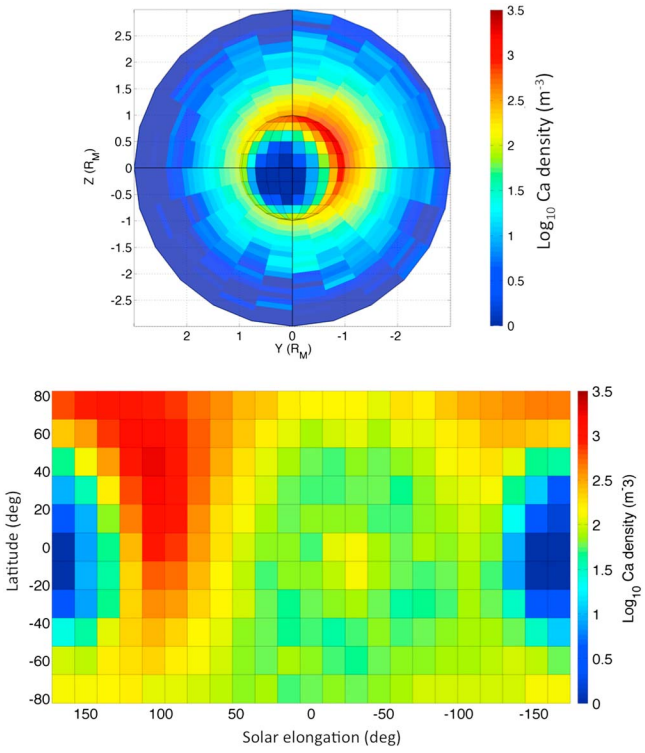

Figure 2. (top) The thermal Ca exosphere of Mercury generated through the photodissociation of the CaO component, as seen from the nightside hemisphere. The *x* and *y* axes are oriented according to the MSO coordinate system (see text); i.e., *z* is positive toward north, *x* is positive toward the Sun, and *y* is positive toward dusk. The exosphere asymmetry between the dawn (on the right) and dusk (on the left) hemispheres is due to the impact vaporization peaking near the dawnside hemisphere. (bottom) Thermal Ca density distribution near the surface. The subradiant solar elongation is 0° at the Sun-planet direction and dawn is at 90°. Ca is preferentially seen on the dawnside because that is where the CaO molecules are preferentially released due to meteoroid impact and subsequently dissociated by the sunlight.

In Figure 2 (top) the spatial distribution of the thermal Ca exosphere (4000 K), generated through the photodissociation of the CaO molecules, seen from above the nightside hemisphere, is presented. The exosphere asymmetry between the dawn (on the right) and dusk (on the left) hemispheres is due to the impact vaporization peaking near the dawnside hemisphere. The highest densities (up to $2 \cdot 10^3$ m^{-3}) are expected near dawn (see Figure 2, bottom); the respective column density of the thermal Ca component, above the region of maximum emission, is up to $2 \cdot 10^5$ cm^2.

The energetic Ca exosphere is presented in Figure 3. Densities up to $2.1 \cdot 10^4$ m^{-3} are expected above the region of maximum emission located in the midnight-to-dawn quadrant. The expected column density is up to $2 \cdot 10^6$ cm^{-2} (see also section 4). The total Ca and CaO vertical profiles above the dawn-to-midnight quadrant are presented in Figure 4.

4. Discussion

As mentioned in section 1, the MESSENGER/UVVS observations revealed that the dominant morphological feature in the Ca exosphere is the dawn enhancement, with variability in source rate, size, and temperature [*Burger et al.*, 2014]. In particular, it was found that the source rate peaks seasonally with values

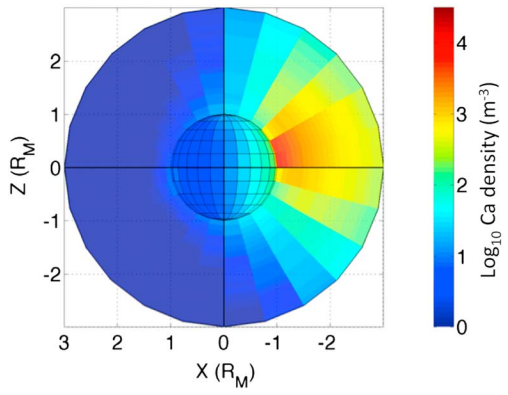

Figure 3. Energetic Ca exosphere (70,000 K) generated through impact vaporization and subsequent dissociation of the CaO molecules, as seen from above the hemisphere centered at the dusk terminator. The *x* and *y* axes are oriented according to the MSO coordinate system (see text); i.e., *z* is positive toward north, *x* is positive toward the Sun, and *y* is positive toward dusk.

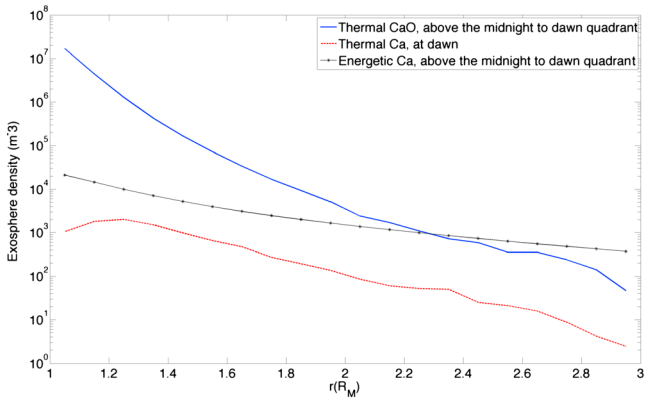

Figure 4. Density profiles of the CaO and the Ca components. The maximum of the both CaO and Ca exospheres is expected in the near surface regions of the midnight-to-dawn quadrant.

up to $3.7 \cdot 10^{23}$ s^{-1} at TAA ~20° and reaches a minimum of $0.4 \cdot 10^{23}$ s^{-1} at TAA ~195°, with the observed dawn-dusk radiance ratio varying in the range of ~5–7. This distribution and variability seemed compatible with the scenario of a Ca-exosphere generation through the MIV process [e.g., *Borin et al.*, 2009; *Christou et al.*, 2015; *Janches et al.*, 2006; *Killen*, 2016; *Pifko et al.*, 2013].

Our results show that the 3-D morphology of the MIV-generated Ca exosphere (both thermal and energetic) is consistent with the UVVS observations; thus, they support the idea that the Ca source peaks near the dawn region [e.g., *Burger et al.*, 2012; *Killen*, 2016] at TAAs in the range of 10°–50°. Nevertheless, the exosphere's energetic Ca source derived from our simulations is significantly lower (by up to 2 orders of magnitude) than the one obtained by *Burger et al.* [2014] through a best fit to the UVVS observations. This discrepancy may be due to the uncertainty in the definition of several parameters used as inputs in our model, the most critical of which are the impact velocity and the ratio between high-energy Ca and the thermal cloud populations generated upon the meteoroid impact to the surface. We also assumed an homogeneous surface composition, although *Weider et al.* [2015] showed that the MESSENGER/XRS-derived maps evidence surface regions by a factor of ~2 denser in Ca, more specifically in the region with also higher Mg and S between 0° and 60° in latitude and 230° and 320° in longitude (called high-magnesium region (HMR) in *Weider et al.* [2015]). If the impact of the meteoroid stream occurs in this region, the expected release would double, as well.

Marchi et al. [2005] have claimed meteoroid impact velocity distributions peaking at higher values than the one proposed by *Cintala* [1992], equal to 20 km/s. In particular, *Marchi et al.* [2005] reported a mean impact velocity for all of their distributions of about 30 km/s but with double peaks, at 30 km/s and at 40 km/s and with tails spanning from about 15 to 80 km/s. Other authors have derived different velocity distributions; for example, the distribution by *Borin et al.* [2009] peaks at velocities lower than 20 km/s and has a less extended high velocity tail. We note, however, that these models apply to meteoroids coming from the Main Belt and not to particles originating from a comet stream. *Killen and Hahn* [2015] argued that the highly repeatable seasonal pattern of Mercury's Ca exosphere seems to exclude the hypothesis that the exospheric feature observed by MESSENGER is due to sporadic impacts widely distributed in frequency (e.g., large meteoroids).

The lack of detailed knowledge on the state of the material during the evolution of the meteoroid impact phenomenon is another problem bringing uncertainty to the current estimations. In the current paper we assume the release of an impact-induced cloud without taking into consideration, for example, possible condensation of solid phases, neither the detailed chemistry within the cloud [e.g., *Berezhnoy and Klumov*, 2008]. So in our model the content of impact-generated Ca in the exosphere will be in a first approximation proportional to the content of this element at the planetary surface. However, condensation of dust grains may lead to significant decreases in the content of nonvolatile elements in the gas phase such as Ca [*Berezhnoy and Klumov*, 2008]. The fraction of the uncondensed Ca in the exosphere varies with the radial dependence of the dust density [*Killen et al.*, 2005]. In addition, in our model we assumed that Calcium is released in the molecular state, preferably in the form of CaO, and that both the meteoroid and Mercury's surface have the same abundance in Ca, equal to 0.035. Moreover, we assumed that the energetic Ca component generated through ionization and dissociation is $<1\%$ of the vapor. These assumptions may

be conservative since experimental works provide evidence of different abundant dissociation products. In particular, *Kurosawa et al.* [2012] conducted shock-compression experiments using a high power laser and carried out in situ spectroscopic observations of silicate vaporization from the end of compression phase to adiabatic expansion to understand energy partitioning process during hypervelocity impacts. Using diopside ($CaMgSi_2O_6$) as a target, these authors observed the change in emission spectrum from strong blackbody radiation into a number of ionic emission lines, e.g., O^+, Ca^+, Mg^+, and Si^+. There are two noteworthy points related to the research by *Kurosawa et al.* [2012]: first, the temperature of the shock-induced cloud was measured to be ranging between 15,000 K and 27,000 K, consistent with the Ca exosphere temperature derived from ground-based spectroscopy; second, although the observed wavelength range covers the regions for molecular band emission of CaO and MgO, these species were not observed. This experimental fact, if applied to the Mercury case, could further sustain the MIV process being a likely process for producing the observed energetic Ca exosphere and the comet Encke stream particles being the main agent of the exosphere's seasonal variation. Indeed, if we assume that at least half of the MIV-generated vapor cloud is released as energetic Ca (instead of 0.85%), the energetic Ca-source rate would become $\sim 10^{23}$, which is comparable to the source rate calculated on the basis of the UVVS data [*Burger et al.*, 2012]. This assumption would bring the column density of the energetic Ca exosphere to the value of $\sim 2 \cdot 10^8$ cm^{-2} (above the surface region of maximum emission) which is very similar to the one estimated by *Killen et al.* [2005] equal to $\sim 1.5 \cdot 10^8$ cm^{-2}.

Another important finding of the MESSENGER observations is the high surface abundance (about 2% according to *Evans et al.* [2012]), especially in the HMR where it approaches 4% [*Weider et al.*, 2015]. In fact, one of the possible compounds of the surface is CaS [*Namur et al.*, 2016], not considered in the *Berezhnoy and Klumov* [2008] study. This hypothesis implies that Ca could be linked to atoms other than oxygen in the MIV-produced cloud; hence, the overall Ca release in the exosphere could be higher than what was previously estimated. *Bennett et al.* [2016], by conducting laboratory measurements on the PSD of CaS powder (an analog for oldhamite) at a wavelength of $\lambda = 355$ nm, showed that the release of Ca from hollows could be substantial even if only 1% CaS is assumed. This low-energy (between 600 and 1400 K) release process would produce a close-to-the-surface exosphere, neither discriminated from the Earth nor from the space, capable of contributing to the thermal Ca-observed distribution. Finally, the Ca release rate could be affected by the specific mineralogy of the surface that should be considered in future simulations.

We note that further experimental work is necessary in order to constrain better the species released through this process and to confirm that impact followed by molecular dissociation produces atomic Ca with an effective temperature of $>$50,000 K. Nevertheless, our resulting morphology of the energetic Ca exosphere, based on the assumptions related to the comet Encke properties, confirms the previous conclusion of other works [e.g.: *Christou et al.*, 2015; *Killen*, 2016] that this is a viable process for the exosphere generation, capable of producing a significant part of the observed hot Ca population in Mercury's exosphere.

According to our model, a seasonal CaO exosphere with density up to $2 \cdot 10^7$ m^{-3} (at altitudes lower than $\sim 0.1\ R_M$) is expected at Mercury. Our simulation results suggest that the CaO column density above the surface region of maximum emission (in the midnight-to-dawn quadrant) is $\sim 4 \cdot 10^8$ cm^{-2}. This estimation is lower than the indicative value proposed by *Killen* [2016], equal to $\sim 2 \cdot 10^9$ cm^{-2}, who used a different model to calculate the MIV-produced flux upon impact. Since the bombardment of Mercury's surface by the comet stream particles (ejected ~10 kyr ago) takes place mainly at TAAs in the range of 10°–50° [*Christou et al.*, 2015, Figure 2, panel 1:1], the lifetime of the MIV-generated CaO exosphere is expected to be equal to ~6.4 days. Whereas the maximum of the thermal CaO exosphere is expected in the near-surface regions of the midnight-to-dawn quadrant, the maximum of the thermal Ca exosphere (generated through the photodissociation of the CaO molecules) is expected at the Northern Hemisphere near dawn. In Figure 4 we plot the density profiles of these components.

The MESSENGER payload did not include a mass spectrometer; hence, it was not possible to detect exospheric molecules. On the contrary, high-resolution mass spectroscopy by the SERENA/STROFIO instrument onboard BepiColombo, the upcoming European Space Agency-Japanese Aerospace Exploration Agency (ESA-JAXA) mission to Mercury, could provide important information on the Ca and Ca-bearing molecule exosphere at Mercury. In order to understand the role of the comet stream particles in the generation of Mercury's calcium exosphere through actual in situ measurements, a dedicated set of observations by

different instruments onboard BepiColombo could be of significant help. This ESA-JAXA mission includes two spacecraft: the orbit of the Mercury Planetary Orbiter (MPO) is polar (periherm ~480 km, apoherm ~1500 km), and it has a period of ~2.30 h, while the Mercury Magnetospheric Orbiter (MMO) has a more eccentric polar orbit (periherm ~600 km, apoherm ~12,000 km). A comparison of the dayside and nightside CaO abundances (see Figure 1), at TAAs in the range from ~20° to 50°, would be useful for understanding the role of meteoroid bombardment in the formation of the exosphere of the planet and, specifically, for evaluating if the considered process efficiency is consistent with the MESSENGER/MASCS/UVVS data. Such observations could be performed primarily with BepiColombo/MPO/ SERENA-STROFIO and PHEBUS instruments. In particular, the nightside observations would be of high importance in the study of the exospheric calcium production through MIV since the contribution of other possible generation processes is expected to be minor.

An investigation with BepiColombo of the Hermean exosphere and of its assumed sources could benefit from an interdisciplinary approach and a synergetic multidata analysis. For example, the possibility to have measurements by the Mercury Dust Monitor (MDM) onboard MMO would help to evaluate the properties of the assumed primary source of the CaO exosphere (i.e., the comet stream particles). MDM would most likely observe the ejecta produced from the surface impacts of the meteoroids, rather than the Encke meteoroids per se (note that the "mass yield," i.e., the ratio of total mass ejected over impactor mass, is typically$\gg$1 [*Koschny and Grün*, 2001]). However, during the passage of Mercury through the comet stream, an enhancement in the MDM detection rate of the ejecta is still likely to be registered. Such an enhancement would confirm the existence of a significant flux of Encke particles during that period. Similar enhancements have been observed recently for the Moon [see *Horányi et al.*, 2015]. The SERENA/STROFIO measurements would provide the actual exosphere density distribution during different orbits of the MPO around the planet. Given that the lifetime of the CaO exosphere is on the order of ~6.4 days and that the MPO orbital period is ~2.3 h, these instruments will have the chance to obtain data with relatively good statistics; at the same time, the SERENA/STROFIO will reveal information also on the actual evolution of the CaO exosphere. Considering the thermal Ca component, observations from the nightside by SERENA/STROFIO would allow the identification of possible dawn-dusk asymmetries in the exosphere. Considering the energetic Ca component, observations by the Mercury Gamma and Neutron Spectrometer (MGNS) along the midnight terminator would allow the determination of the elemental compositions and, therefore, the identification of regions of possibly modified surface composition due to meteoroid impacts.

5. Conclusions

In this paper we provided for the first time the spatial distribution of Mercury's CaO exosphere generated through MIV caused by the comet Encke's stream particles intersecting the orbit of Mercury at TAAs in the range of 10°–50°.

The results of this work are summarized as follows:

1. The generation of seasonal CaO exosphere with densities up to $2 \cdot 10^7$ m^{-3} is expected. Such an exosphere is not symmetric: the maximum surface release is expected on the dawnside-nightside hemisphere, near the equator, because that is where the comet stream particles preferentially impact the planet's surface according to the model by *Christou et al.* [2015].
2. An exospheric energetic Ca component, derived from the dissociative ionization and neutralization of CaO is expected above the same region.
3. The spatial distribution of the thermal Ca exosphere generated by photoionization of the CaO molecules in sunlight is expected to be asymmetric exhibiting local maxima in the near dawn regions.
4. While the simulated Ca distribution is in good agreement with the MESSENGER/MASCS/UVVS observations, the derived emission rate is up to one tenth of the observed abundances. Our estimation of this energetic population depends strongly on the assumed properties of the MIV process taking place at the surface of Mercury.

We note that in the current work we assumed a conservative source rate for the MIV-derived exospheric populations. Although our knowledge on the details of this mechanism is currently limited, experiments by *Kurosawa et al.* [2012] provide evidence that a significant amount of energetic atomic Ca can be released through the dissociative ionization mechanism upon high-velocity impacts. If this is the case of Mercury, our model results would further support the MIV process being the culprit for producing the observed energetic

Ca exosphere and the comet Encke stream particles being the main agent of the exosphere's seasonal variation.

A synergetic multidata analysis of the Hermean neutral environment and of its assumed sources with BepiColombo would provide important feedback on the role of the Encke micrometeoroids in the Ca-exosphere generation. The properties of the assumed primary source of the CaO exosphere could be investigated on the basis of the MMO/MDM measurements of the ejecta produced from the surface impacts of the meteoroids. The exosphere density distribution and its evolution during different orbits of the MPO around the planet will be provided by the MPO/SERENA/STROFIO measurements. Observations from the nightside by MPO/SERENA/STROFIO would provide a unique opportunity to identify possible dawn-dusk asymmetries in the Ca exosphere. Last, the MPO/MGNS measurements along the midnight terminator would indicate regions of possibly modified surface composition due to meteoroid impacts.

Acknowledgments
This paper is financially supported by ASI (Italian Space Agency) under contract "SERENA" I/081/09/0. The results presented in this paper are outcome of theoretical simulations, and no analysis of experimental data has taken place. All numerical data produced through the simulations can be accessed through the following link: https://github.com/giamihai/Ca_exosphere.

References

Berezhnoy, A. A. (2013), Chemistry of impact events on the Moon, *Icarus*, *226*, 205–211, doi:10.1016/j.icarus.2013.05.030.
Berezhnoy, A. A., and B. A. Klumov (2008), Impacts as sources of the exosphere on Mercury, *Icarus*, *195*, 511–522, doi:10.1016/j.icarus.2008.01.005.
Bennett, C. J., J. L. McLain, M. Sarantos, R. D. Gann, A. DeSimone, and T. M. Orlando (2016), Investigating potential sources of Mercury's exospheric calcium: Photon-stimulated desorption of calcium sulfide, *J. Geophys. Res. Planets*, *121*, 137–146, doi:10.1002/2015JE004966.
Bida, T. A., R. M. Killen, and T. H. Morgan (2000), Discovery of Ca in Mercury's atmosphere, *Nature*, *404*, 159–161, doi:10.1038/35004521.
Borin, P., G. Cremonese, F. Marzari, M. Bruno, and S. Marchi (2009), Statistical analysis of micrometeoroids flux on Mercury, *Astron. Astrophys.*, *503*, 259–264, doi:10.1051/0004-6361/200912080.
Burger, M. H., R. M. Killen, W. E. McClintock, R. J. Vervack Jr., A. W. Merkel, A. L. Sprague, and M. Sarantos (2012), Modeling MESSENGER observations of calcium in Mercury's exosphere, *J. Geophys. Res.*, *117*, 0L11B, doi:10.1029/2012JE004158.
Burger, M. H., R. M. Killen, W. E. McClintock, A. W. Merkel, R. J. Vervack Jr., T. A. Cassidy, and M. Sarantos (2014), Seasonal variations in Mercury's dayside calcium exosphere, *Icarus*, *238*, 51–58, doi:10.1016/j.icarus.2014.04.049.
Cintala, M. J. (1992), Impact-induced thermal effects in the lunar and Mercurian regoliths, *J. Geophys. Res.*, *97*, 947–973, doi:10.1029/91JE02207.
Christou, A. A., R. M. Killen, and M. H. Burger (2015), The meteoroid stream of comet Encke at Mercury: Implications for MErcury Surface, Space ENvironment, GEochemistry, and Ranging observations of the exosphere, *Geophys. Res. Lett.*, *42*, 7311–7318, doi:10.1002/2015GL065361.
Evans, L. G., et al. (2012), Major-element abundances on the surface of Mercury: Results from the MESSENGER Gamma-Ray Spectrometer, *J. Geophys. Res.*, *117*, E00L07, doi:10.1029/2012JE004178.
Huebner, W. F., and J. Mukherjee (2011), Photo Rate Coefficient Database. [Available at http://phidrates.space.swri.edu.]
Horányi, M., J. R. Szalay, S. Kempf, J. Schmidt, E. Grün, R. Srama, and Z. Sternovsky (2015), A permanent, asymmetric dust cloud around the Moon, *Nature*, *522*, 324–326, doi:10.1038/nature14479.
Janches, D., C. J. Heinselman, J. L. Chau, A. Chandran, and R. Woodman (2006), Modeling the global micrometer input function in the upper atmosphere observed by high power and large aperture radars, *J. Geophys. Res.*, *111*, A07317, doi:10.1029/2006JA011628.
Killen, R. M. (2016), Pathways for energization of Ca in Mercury's exosphere, *Icarus*, *268*, 32–36, doi:10.1016/j.icarus.2015.12.035.
Killen, R. M., and J. M. Hahn (2015), Impact vaporization as a possible source of Mercury's calcium exosphere, *Icarus*, *250*, 230–237, doi:10.1016/j.icarus.2014.11.035.
Killen, R. M., and W.-H. Ip (1999), The surface bounded atmospheres of Mercury and the Moon, *Rev. Geophys. Space Phys.*, *37*, 361–406, doi:10.1029/1999RG900001.
Killen, R. M., T. A. Bida, and T. H. Morgan (2005), The calcium exosphere of Mercury, *Icarus*, *173*, 300–311, doi:10.1016/j.icarus.2004.08.022.
Killen, R. M., et al. (2007), Processes that promote and deplete the atmosphere of Mercury, *Space Sci. Rev.*, *132*, 433–509, doi:10.1007/s11214-007-9232-0(Mercury).
Koschny, D., and E. Grün (2001), Impacts into ice-silicate mixtures: Ejecta mass and size distributions, *Icarus*, *154*, 402–411, doi:10.1006/icar.2001.6708.
Kurosawa, K., et al. (2012), Shock-induced silicate vaporization: The role of electrons, *J. Geophys. Res.*, *117*, E04007, doi:10.1029/2011JE004031.
Lee, N., et al. (2012), Measurements of freely-expanding plasma from hypervelocity impacts, *Int. J. Impact Eng.*, *44*, 40–49, doi:10.1016/j.ijimpeng.2012.01.002.
Mangano, V., A. Milillo, A. Mura, S. Orsini, E. De Angelis, A. M. Di Lellis, and P. Wurz (2007), The contribution of impulsive meteoritic impact vapourization to the Hermean exosphere, *Planet. Space Sci.*, *55*(11), 1541–1556, doi:10.1016/j.pss.2006.10.008.
Marchi, S., A. Morbidelli, and G. Cremonese (2005), Flux of meteoroid impacts on Mercury, *Astron. Astrophys.*, *431*, 1123–1127, doi:10.1051/0004-6361:20041800.
McClintock, W. E., and M. R. Lankton (2007), The Mercury atmospheric and surface composition spectrometer for the MESSENGER mission, *Space Sci. Rev.*, *131*, 481–521, doi:10.1007/s11214-007-9264-5.
Mura, A., P. Wurz, H. I. M. Lichtenegger, H. Schleicher, H. Lammer, D. Delcourt, A. Milillo, S. Orsini, S. Massetti, and M. L. Khodachenko (2009), The sodium exosphere of Mercury: Comparison between observations during Mercury's transit and model results, *Icarus*, *200*(1), 1–11, doi:10.1016/j.icarus.2008.11.014.
Namur, O., B. Charlier, F. Holtz, C. Cartier, and C. McCammon (2016), Sulfur solubility in reduced mafic silicate melts: Implications for the speciation and distribution of sulfur on Mercury, *Earth Planet. Sci. Lett.*, *448*, 102–114, doi:10.1016/j.epsl.2016.05.024.
Pifko, S., D. Janches, S. Close, J. Sparks, T. Nakamura, and D. Nesvorny (2013), The meteoroid input function and predictions of mid-latitude meteor observations by the MU radar, *Icarus*, *223*, 444–459, doi:10.1016/j.icarus.2012.12.014.
Sidis, V. (1989), Theory of dissociative charge exchange in ion–molecule collisions, *J. Phys. Chem.*, *93*(25), 8128–8138, doi:10.1021/j100362a003.

Solomon, D., J. Lehmann, J. Thies, T. Schäfer, B. Liang, B. J. Kinyangi, E. Neves, J. Petersen, F. Luizão, and J. Skjemstad (2007), Molecular signature and sources of biochemical recalcitrance of organic C in Amazonian dark earths, *Geochim. Cosmochim. Acta*, *71*(9), 2285–2298, doi:10.1016/j.gca.2007.02.014.

Starks, M. J., D. L. Cooke, B. K. Dichter, L. C. Chhabildas, W. D. Reinhart, and T. F. Thornhill III (2006), Seeking radio emissions from hypervelocity micrometeoroid impacts: Early experimental results from the ground, *Int. J. Impact Eng.*, *33*, 781–787, doi:10.1016/j.ijimpeng.2006.09.044.

Weider, S. Z., et al. (2015), Evidence for geochemical terranes on Mercury: Global mapping of major elements with MESSENGER's X-Ray Spectrometer, *Earth Planet. Sci. Lett.*, *416*, 109–120, doi:10.1016/j.epsl.2015.01.023.